J. Astrophys. Astr. (2001) 22, 251–262

Deconvolution of Wide-field Images from a Non-Coplanar T-Array

K. Golap[1] & N. Udaya Shankar[2,1].
[1] *Department of Physics, University of Mauritius, Reduit, Mauritius.*
[2] *Raman Research Institute, Sadashivanagar, Bangalore 560080, India.*

Received 2001 August 21 ; accepted 2001 October 16*

Abstract.

Deconvolution of wide-field images is a well-known problem with many interesting algorithms. In this paper we describe the solution developed for deconvolving wide-field images from the Mauritius Radio Telescope (MRT). MRT is a non-coplanar, Fourier synthesis T array operating at 151.5 MHz. The non-coplanarity of the MRT produces dirty images that are convolved by a position dependent point spread function (PSF). This paper mainly focuses on the methods developed for estimating the PSF of the array from the dirty images and translating the PSF estimated at a given declination to the PSF at any another declination.

1. Introduction

The Mauritius Radio Telescope (MRT) is a Fourier synthesis T-shaped array with an East-West (EW) arm of length 2048 m having 1024 helical antennas. The South (S) arm consists of a rail line of length 880m and 16 movable trolleys each with four helical antennas. The 1024 helices in the EW arm are divided into 32 groups of 32 helices each. The local terrain is rocky and uneven, especially along the EW arm with height differences of up to 35 m. To minimize the problems of non-coplanarity, it was decided to level the EW arm in multiples of 64 m (32λ) so that the antennas in each group will be at the same height. Each trolley in the S arm constitutes one S group. A detailed description of the telescope is to be found in Golap *et al* (1998).

The 48 group outputs are amplified, heterodyned to 30 MHz in the field and brought separately to the observatory building via coaxial cables. In the observatory, the 48 group outputs are further amplified and down-converted to a second IF of 10.1 MHz.

The 32 EW and 16 S group outputs are fed into a 32×16 complex, 2-bit 3-level

*Although this paper was accepted only on 16 October, we have included it because this issue was delayed due to other reasons.

digital correlator sampling at 12 MHz. The 512 complex visibilities are integrated and recorded at intervals of 1s. At the end of 24 hours of observations the trolleys are moved to a different position and new visibilities are recorded. The S baselines are sampled with a spacing of 1m, which is half a wavelength at 150 MHz. A minimum of 60 days of observing are needed to obtain the visibilities up to 880 m spacing.

The visibilities measured by an interferometer of baseline $\vec{b} \equiv (u, v, w)$ is given by Thompson *et al* (1986):

$$\tilde{V}(u,v,w) = \int\int \frac{A(l,m)B(l,m)}{\sqrt{1-l^2-m^2}} \exp(-i(lu+mv+nw))dldm. \quad (1)$$

where A(l,m) is the amplitude response of the array, B(l,m) is the sky brightness distribution and l,m,n are the direction cosines.

Let $B'(l,m) \equiv \frac{B(l,m)A(l,m)}{\sqrt{1-l^2-m^2}}$. Then the above equation becomes

$$\tilde{V}(u,v,w) = \int\int B'(l,m) \exp(-i(lu+mv+w\sqrt{1-l^2-m^2}))dldm. \quad (2)$$

where $B'(l,m)$ is the modified brightness distribution. For planar arrays this relationship can be simplified to a 2-dimensional Fourier transform.

The *u,v* coverage of MRT can be thought of as a pleated sheet, extended in both *u* and *v*, with discrete steps in *w* (height) as we move from one EW group to the other at a different height. As we are imaging a very large field of view ($\approx 60'$), the approximate coplanar approach wherein the phase term due to the heights is assumed to be a constant over the synthesized field of view is invalid. Thus for MRT, a 3D imaging is required.

To avoid the grating response of the EW array, imaging is presently carried out on the meridian (Golap *et al* 1998). For meridian transit imaging, we transform the visibilities using a Fast Fourier Transform (FFT) along the regularly sampled *v* axis, apply a Direct Fourier Transform (DFT) along the *w* axis and finally sum along *u* to obtain the image on the meridian. A DFT on *w* is required as the sampling is not uniform. The direct transform corrects every term along the zenith angle on the meridian for the group heights. This is equivalent to phasing the groups to a common (and artificial) 2D plane and results in a dirty image convolved by a position dependent PSF.

We discuss in this paper a technique developed to deconvolve wide field images made using the MRT to obtain images with reasonable dynamic ranges ($\approx 1:100$). Our deconvolution method is based on the conventional CLEAN algorithm (Clark *et al* 1980; Hogbom 1974; Schwartz *et al* 1978). This needs knowledge of the Point Spread Function (PSF) of the array. The next section discusses the effect of the non-coplanarity of the array on the PSF and shows that it is a function of declination. Section 3 discusses the need and the method for the estimation of the PSF from the dirty images. Section 4 describes an algorithm to generate PSFs for

different declinations from the estimate at a given declination. Section 5 describes the application of the method developed to the deconvolution of images made using MRT for a low resolution survey ($17' \times 13'\sec(\delta - \phi)$).

2. The effect of non-coplanarity on the PSF

The PSF of a T-array is generally a complex function with a non-zero imaginary part. The real part of the PSF of a uniformly illuminated T- array is the same as that of a cross (Christiansen *et al* 1985). We use only the real beam and the corresponding real image for deconvolution. However, the imaginary part of the PSF is required when generating the PSF for a planar array with a non uniform illumination and for a non-coplanar array (Dwarakanath *et al* 1990).

Both the EW and the S arrays of the MRT are non-coplanar. The height profile of the EW array is shown in the Fig. 1.

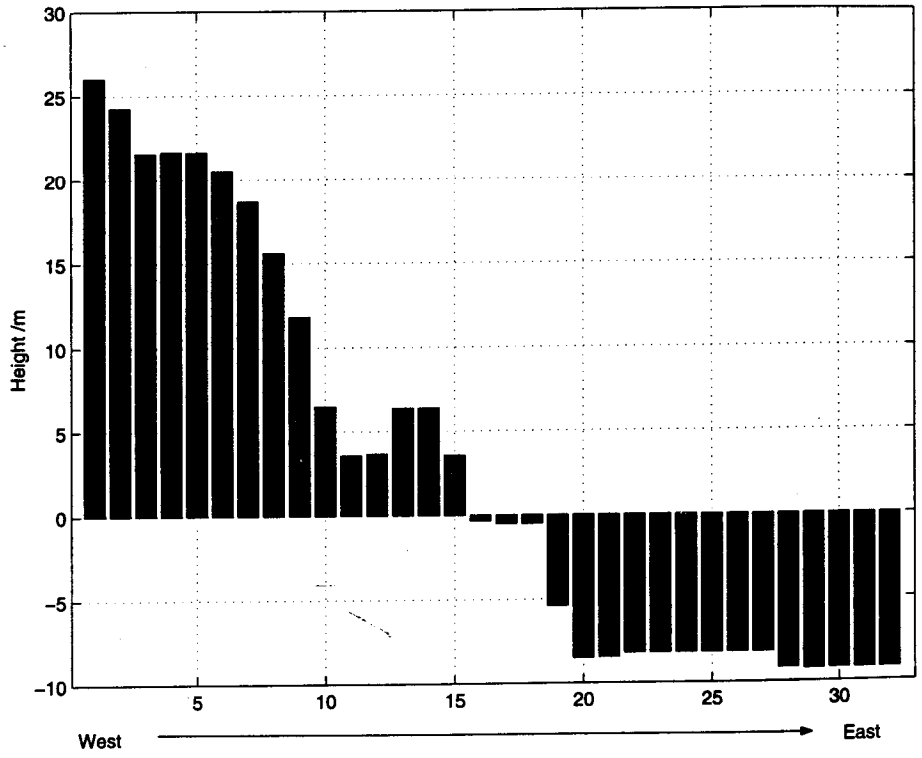

Figure 1. A plot showing the height profile of the EW array. Each bar represents a 64 m long EW group with 32 helices. The profile runs from west to east end.

An abandoned old railway line running North-South was rebuilt for use as the South arm. This arm slopes downwards at about $\frac{1}{2}^\circ$ to the horizontal till about 655 m, and then slopes upwards at about 1° to the horizontal. Visibilities measured

from these two parts are treated separately while transforming. The slope is taken into account by assuming an instrumental zenith appropriate to the slope of the track. While combining contributions from different parts we introduce necessary corrections to get an instrumental zenith equal to the latitude of the place. This treatment of visibilities does not result in a PSF substantially different from that of a co-planar T array. The deviation of the PSF of the MRT from that of a co-planar T array is mainly due to the non-coplanarity of the EW array.

Let us consider an EW group which is at a height h, from the NS array. Signal from a point source on the meridian, with a zenith angle (za) reaches the EW group with an extra path difference of $h \times \cos(za)$. While imaging, one compensates for a phase shift due to this path difference at each zenith angle along the meridian. This is carried out for all the baselines used for imaging. This results in the sidelobe of a source at za_1 appearing at za_2, getting compensated by a height phase equivalent to that at za_2. This causes a reduction in the level of the sidelobe at za_2. However the sidelobe around za_1 peaks at some other hour angle (HA) away from the meridian. Thus sidelobes of a source peaks at an RA which is different from its transit time. The position and the strength of the sidelobe depends upon how far it is from the source, the source declination and the EW height distribution. The dirty image around the source MRC2155-699 shown in the Fig. 2 clearly illustrates this effect.

The Fourier inversion of the visibilities measured by a non-coplanar array gives the function $F(l,m,n)$ (see, e.g. Cornwell *et al* 1992).

$$F(l,m,n) = \left[B'(l,m,n)\delta(\sqrt{1-l^2-m^2}-n)\right] * P(l,m,n), \qquad (3)$$

where $P(l,m,n)$ is the 3-D PSF. Equation(3) can be simplified to

$$F(l,m) = \int B'(l_o,m_o)P(l-l_o,m-m_o,\sqrt{1-l^2-m^2}-\sqrt{1-l_o^2-m_o^2})dl_o dm_o. \qquad (4)$$

Now let us consider an isolated point source in the sky. As the point source drifts in the sky transiting the meridian, its direction cosines l', m' change with the HA. The dirty image, when the point source is at l', m', is given by

$$F_{PSF}^{(l',m')}(l,m) = k \int \delta(l_o - l', m_o - m') \times P(l-l_o,m-m_o,\sqrt{1-l^2-m^2}-\sqrt{1-l_o^2-m_o^2})dl_o dm_o, \qquad (5)$$

$$= kP(l-l',m-m',\sqrt{1-l^2-m^2}-\sqrt{1-l'^2-m'^2}). \qquad (6)$$

For $l = 0$,

$$F_{PSF}^{(l',m')}(0,m) = kP(-l',m-m',\sqrt{1-m^2}-\sqrt{1-l'^2-m'^2}). \qquad (7)$$

Close to the meridian, m' can be simplified to $\sin(-za)$. Then the PSF is a one dimensional function F(0,m) for various values of l' given by

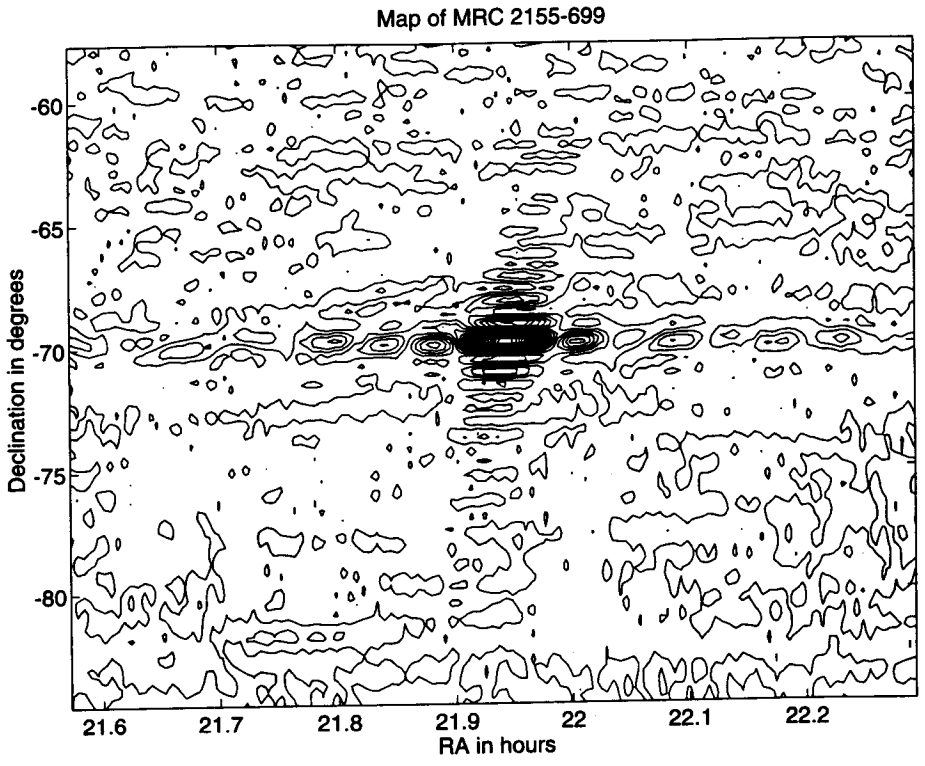

Figure 2. Dirty image around the source MRC2155-699. The twisted response of the array due to the non-coplanarity is clearly seen.

$$F_{PSF}^{(l',m')}(0,m) = kP(-l', m-m', \sqrt{1-m^2} - \sqrt{1-l'^2-m'^2}), \quad (8)$$

$$= kP(-l', sin(za') - sin(za), cos(za) - cos(za')). \quad (9)$$

Thus the two-dimensional PSF at m due to a point source at l', m' is not merely a function of $m - m'$ but also depends on m.

Thus the PSF will have different shapes depending on where the point source is centered. This implies that for deconvolution of the antenna response from the 2-D image we need different functions which depend upon the Zenith Angle of the source being deconvolved.

2.1 *Estimation of the PSF*

In the present work the imaging is restricted to making 1-D scans along the meridian. The 2-D image is time stacks of these 1-D scans. As a point source drifts across the meridian the 1-D stacks will give the point spread function. The T array

is used in a correlation mode in which the EW array is multiplied with the NS array. Thus the observed PSF is that of the NS array multiplied by the PSF of the EW array. Since the PSF and the aperture illumination are a Fourier transform pair, the PSF can be generated from the aperture illumination.

At MRT correlation of signals from groups of helices are performed. There are 32 helices in each of the EW groups and 4 helices in each of the NS groups. The calibration procedure used (Golap *et al* 1998) gives the phases and amplitudes of a group. The illumination pattern within each group is not estimated. This sets a limit to the extent of the PSF that can be estimated from the illumination pattern. For example, in the low resolution survey, only 8 central groups in the EW arm and trolley positions up to 178 m in the NS are used (Golap 1998). Thus using the aperture illumination from our calibration, we can estimate the PSF up to 4 sidelobes on each side of the main beam along the RA direction and 89 sidelobes along the declination on the meridian. The image will have a dynamic range of ≈ 12 if such a PSF is used for deconvolution (assuming a sinc pattern for the PSF). Hence CLEANing point sources stronger than 12 Jy would leave residues higher than 1 Jy in the final image; 1 Jy being the approximate noise level (1σ) of the low resolution survey. Hence we use the dirty image around a strong point source to estimate the PSF with an extent larger than four sidelobes on either side of the main lobe.

To achieve a dynamic range of, say, around 50 the PSF should have an extent of at least 16 sidelobes on either side of the main beam. In other words we need a field of $7.5^\circ \times 7.5^\circ$ with the point source in the centre. However such a field will have other sources apart from the point source under consideration. Such sources (especially if they lie along the same RA or declination) may not be distinguishable from the side lobes. Hence we may generate an unsatisfactory PSF. This effect can be minimised by averaging the PSFs estimated using point sources at different declinations.

The sky coverage of the low resolution survey is 18:00 to 24:00 hrs and 00:00 to 05:00 hrs in RA and from -70° to -10° in declination. There are not many strong point sources in this field to obtain the PSF at different declinations. The flux density of the strongest point source MRC1932-464 in this field is $\approx 80 Jy$ and is just strong enough to determine the PSF.

The process of averaging of several PSFs of weaker sources will improve the estimation process. However since the PSF of the MRT is declination dependent it is not straight forward to sum the PSFs estimated at different declinations. This can be carried out if we are able to generate the PSF at a given declination δ_1 from the PSF estimated at some other declination δ_0. The next section discusses this.

3. Declination Shift Algorithm

If one plots the PSF of a planar array as a function of RA and $\sin(za)$, the declination scan of the PSF remains invariant with the zenith angle. The RA scan of

the PSF gets stretched by $\sec(\delta)$ as one moves to sources at different declinations. Because of the ease that m or $\sin(za)$ coordinate offers, the images were uniformly sampled in the $\sin(za)$ domain and the (RA, $\sin(za)$) coordinate system was used for the PSF and dirty images.

To sum the PSF estimated by sources at different declinations, we should be able to generate the PSF at any given declination δ_1 from the PSF at some other declination δ_0.

Let us consider the PSF of a source centered at δ_0, with its zenith angle $za_0 = \delta_0 - \phi$ and $m_0 = -\sin(za_0)$, where ϕ is the latitude of the telescope.

Any RA cut of the PSF, say at $m = m'_o$, which is different from the m of the source, is complex with non zero imaginary part. While imaging this declination, a phase correction corresponding to heights seen at the point $m = m'_o$ would have been put in. A Fourier transformation of this cut gives the "combined" spatial frequency response of the EW antennas used. Since in the EW×NS mode there are no redundant baselines, when the number of Fourier components estimated is equal to integral number of the EW groups, each Fourier component can be thought of as arising from a given EW group. Assuming that there is only one point source in the field of view, the entire signal comes from that source. Hence the Fourier components have been given a height correction due to m'_o, ($\Phi_{m'_o}(h) = h \times \cos(za'_o) = hn'_o$) while the signal has a phase due to height as seen at m_o ($\Phi_{m_o}(h) = hn_o$), where h is the height of the EW group corresponding to the Fourier component we are considering. Therefore there is a residual phase error corresponding to the path difference of $(\Phi_{m_o}(h) - \Phi_{m'_o}(h))$ in each Fourier component.

The process of declination shift consists of replacing these residual phase errors in Fourier components with the values expected if the source were centered at δ_1, which are proportional to $\Phi_{m_1}(h) - \Phi_{m'_1}(h)$. After this phase rotation the Fourier components are inverse transformed. This procedure is repeated across the declination range of the PSF to reconstruct it at δ_1. Reconstruction of the PSF at δ_1 also requires the RA section to be stretched or compressed to have a width proportional to $\sec(\delta_1)$.

The PSF at any declination can be made to look like the one obtained using a coplanar array by removing the residual phase errors mentioned above. This is equivalent of correcting for the heights at the declination of the source rather than the declination of the sidelobe. This would ensure that all the sidelobes, along the declination, peak on the meridian and the one dimensional stacks of the images would look similar to the one obtained with an array in which all the EW groups are at the same height. Then a pseudo PSF can be obtained by taking the real part of the complex product of the two one dimensional cuts across RA and declination. This is a reasonable approach since in the correlation mode one produces the 2-D response by multiplying the response of the EW and NS arrays (Dwarakanath *et al* 1990). Such a two dimensional PSF can later be transformed to the PSF of MRT at any declination by introducing the residual phase errors in its Fourier transform.

4. Low Resolution PSF and CLEAN

The declination shift algorithm was used to generate the PSF required for CLEANing the low resolution images ($17' \times 13'\sec(\delta - \phi)$). As already mentioned a low resolution survey using the observations covering the NS baselines up to 178 m has been carried out. To have nearly a symmetric beam for the images, data for baselines only with the central 512 m of the EW arm was used. The sky coverage of the low resolution survey is 18:00 to 24:00 hr and 00:00 to 05:00 hr in RA and from $-70°$ to $-10°$ in declination. The estimated noise in the image is around 1 Jy and is confusion limited (Golap 1998).

In the field of view of the survey four brightest point sources (flux density range 35-120 Jy) were used for estimating the PSF.

The following points were considered while constructing the PSF.

- The sources chosen are far from the Galactic plane but their fields are not devoid of large scale structures. We used a dirty image without zero spacing for the estimation of the PSF and also for the deconvolution. As regards the large scale structures in the PSF, we did not take any additional precautions. However, the averaging, of four regions for the estimation of the PSF, reduced the effect of the large scale structures from any single field.

- Interference affects the PSF estimation. An inspection of the images around the sources chosen did not show any interference.

After selecting a region $\approx 7.5° \times 7.5°$ around the sources. The following procedure was used to estimate the PSF:

1. Select a region with an extent of n sidelobes around the main beam. To get a dynamic range of d in an image with an *rms* noise σ, source should have a strength of at least $\sigma \times d$. If the PSF is approximately a sinc function, n should satisfy the condition $n < \frac{d}{\pi}$.
2. Subtract all identifiable sources in the field of view other than the central source of interest. For this we adopted a source detection program which identifies high points in the selected regions of the dirty image where gradients are negative in all directions, fits approximate RA and declination beams in the first step and a two dimensional beam later. Visual inspection is carried out using the apriori information available about the region from the Molongolo Reference Catalogue (MRC) (Large *et al* 1981) to ensure that the sidelobes of the central source are not mistaken for independent sources.
3. Phase rotate the Fourier transforms of the complex RA cuts of the above region to obtain the pseudo PSF of the array at zenith. This is nothing but the PSF of the MRT with its EW groups at the same height. While Fourier transforming an RA scan, its extent is chosen to give integral number of points within each group. Helices within each EW group

are at the same height. Hence each Fourier component will have one representative height

4. Repeat the steps 1, 2 and 3 for the four regions and average the pseudo PSF with suitable weighting factors.

5. Obtain two one dimensional complex scans of the above function with the source at the centre. The real part of the complex product of these two scans gives an improved average pseudo PSF.

6. While deconvolving this is transformed to the true PSF of MRT at the declination of interest using the declination shift algorithm.

We used the task APCLN in AIPS for deconvolution. The PSF at zenith generated by averaging PSFs of four sources with suitable weightages is shown in the Fig. 3. The PSF generated by cross multiplying the complex scans taken from this average PSF is shown in Fig. 4. The noise in the off-axes regions in this PSF is much lower than that shown in Fig. 3. The CLEANed image of Fornax A region is shown in Fig. 5. The source which is just below Fornax A is MRC0320-389 which has a flux density $\approx$ 4 Jy. The peak flux of the of the Fornax A is $\approx$ 290 Jy/beam. This gives a dynamic range $\approx$ 70.

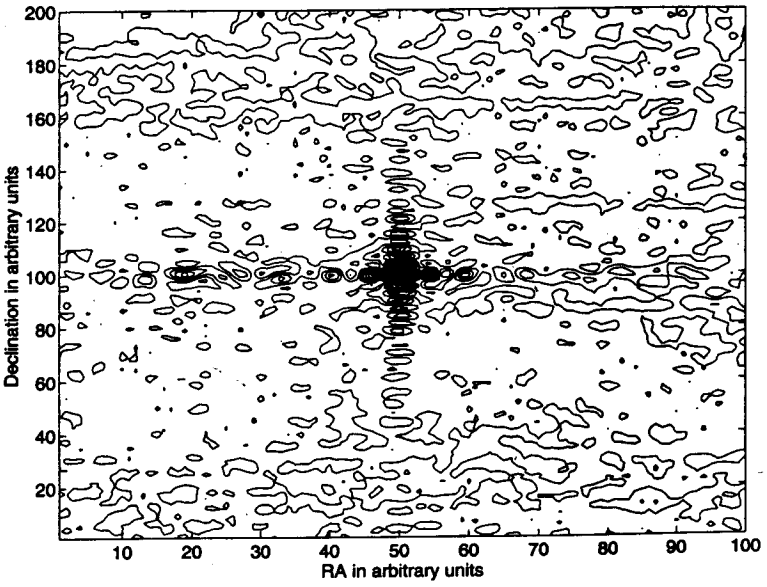

Figure 3. PSF at zenith generated by averaging the PSF of four sources. Note the noise in the off-axes region when compared to the PSF shown in Fig. 4.

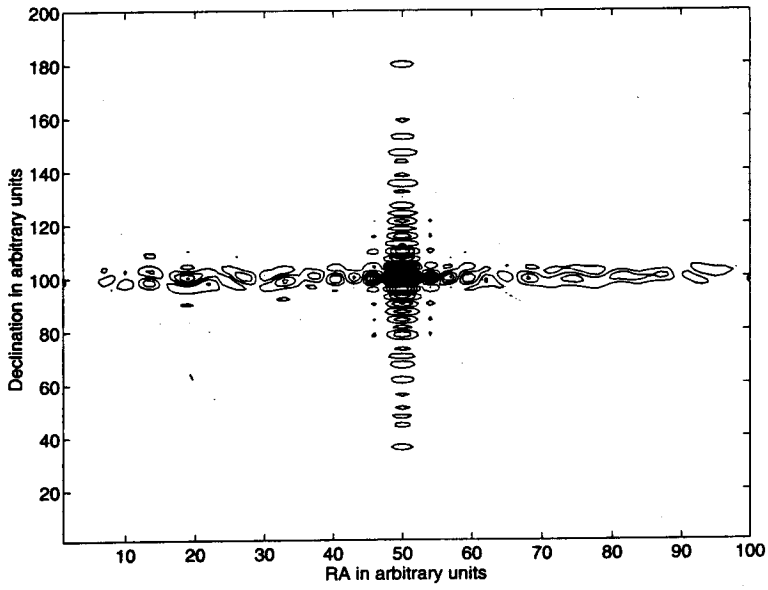

Figure 4. PSF generated by cross-multiplying the 1-D complex scans taken from the PSF of Fig.3

The dirty images from the low resolution survey have been CLEANed using the technique demonstrated here. The low resolution survey details will be discussed in a separate paper.

5. Conclusions

We have developed a technique to translate the position dependent PSF of a non-coplanar T-array. Employing this technique gainfully we are able to estimate the PSF required for deconvolution from the dirty images minimising the effects of off-axes sources by averaging the PSF of several sources. We have demonstrated the technique developed here by deconvolving a low resolution MRT image in the Fornax A region. This is one of the strong sources in the field of view of our survey. We have been able to achieve a dynamic range of 70, close to the axes of the source and a much higher dynamic range away from the axes. This technique has been put to use in preparing a low resolution survey of the southern sky. The sky coverage of the low resolution survey is 18:00 to 24:00 hr and 00:00 to 05:00 hr in RA and from $-70°$ to $-10°$ in declination. The estimated noise in several fields is ≈ 1 Jy. This is close to the expected sensitivity which is confusion limited. The next logical step is to develop techniques similar to hybrid imaging (Pearson *et al* 1997) for estimating antenna gains using these images as the first approximation for the field of view and hence re-calibrate the measured visibilities.

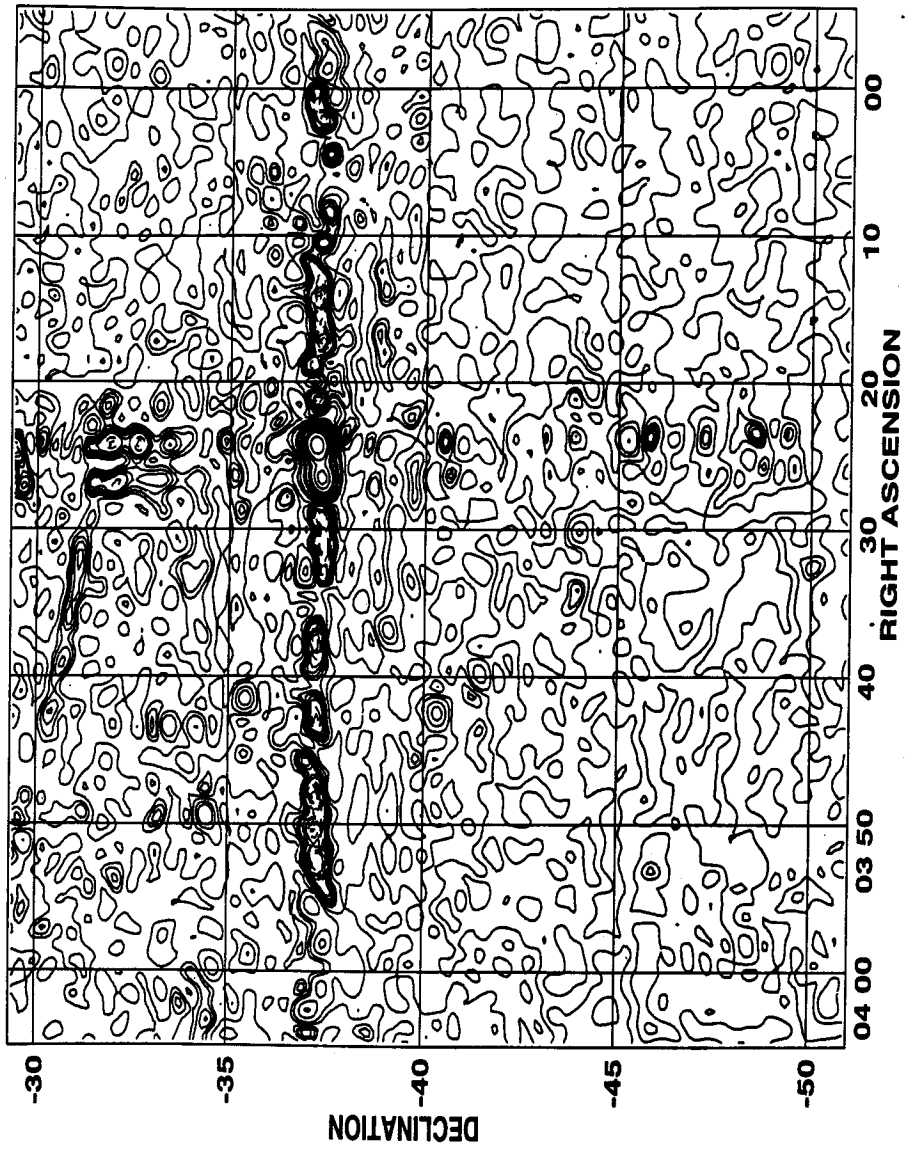

Figure 5. Fornax-A cleaned with a beam generated with 4 point sources

6. Acknowledgments

The MRT is operated jointly by the Raman Research Institute, Bangalore; Indian Institute of Astrophysics, Bangalore and the University of Mauritius. K.Golap wishes to thank the many people that helped but specifically would like to mention and dedicate this work to R. Somanah, H.A. Aswathappa and G. N. Rajasekar. R. Somanah helped in staving the many adminsitrative crises and the 'urgent paper work' that came along often. H.A.Aswathappa, specially, and G.N.Rajasekar provided dedicated technical support; which often meant trying to repair amplifiers and the correlator at 2:00 Am, after working in the field during the day.

References

Christiansen, W.N., and Hogbom, J.A., *"Radio Telescopes"*, Cambridge University press, 1985.

Clark, B.G., 1980, *Astron. Astrophys.*, **89**, 377.

Cornwell, T.J., Perley, R.A., 1992, *Astron. Astrophys.*, **261**, 353C.

Dwarkanath, K.S., Deshpande, A.A., Udaya Shankar, N., 1990, *J. Astrophys. Astr.*, **11** , 311.

Golap, K., *"Synthesis Imaging At 151.5 MHz Using The Mauritius Radio Telescope"*, Ph.D. Thesis, Dept. of Physics, University Of Mauritius, 1998.

Golap, K., Udaya Shankar, N., Sachdev, S., Dodson, R., Sastry, Ch. V., 1998, *J. Astrophys. Astr.*,**19**, 35.

Hogbom, J., 1974, *Astr. Astrophys. Suppl.*, **15** , 417.

Large, M. I., Mills, B. Y., Little, A. G., Crawford, D. F., Sutton, J. M., 1981, *MNRAS*, **194**, 693.

Pearson, T.J., Readhead, A.C.S., 1984, *ARA&A* , **22**, 97.

Schwartz, U.J., 1978, *Astron. Astrophys.*, **65**, 345.

Thompson, A. R., Moran, J. M., Swenson, G. W. Jr. *"Interferometry and Synthesis in Radio Astronomy"*. John Wiley and Sons, 1986.